

LIDAR-BASED FLOOD HAZARD SIMULATION IN NORTHEASTERN LUZON RIVER BASINS, PHILIPPINES

Januel P. Floresca ⁽¹⁾

¹ Isabela State University, Echague, Isabela, Philippines
Email: januelpf@gmail.com; januelpf@yahoo.com.ph

KEYWORDS: Digital terrain model, digital surface model, HEC-HMS, HEC-RAS, Aunugay River Basin

ABSTRACT: This paper aims to show the accuracy of a new flooding simulation system, based on LiDAR-derived DTM and DSM, capable of predicting impacts to agriculture, aquatic, forestry, natural resources (AAFNR) and properties at specified rainfall scenarios (5-, 25-, and 100-year rainfall return period (RRP)). Covering 6,087.48 km² processed LiDAR data in 10 selected river basins (RBs) in Northeastern Luzon, accuracy DTM and features extracted from DSM had passed the allowable 2.0 m RMSE. The HEC-HMS models obtained satisfactory efficiency test values: Pearson correlation coefficient (r^2) of 0.89-0.97 and Nash-Sutcliffe Error (NSE) of 0.77-0.96 which were close to 1.00; more negative percent bias (PBIAS); and low standard deviation ratio (RSR) of 0.19-0.48 indicating an almost perfect match between simulated and observed outflows. Flood heights accuracy was satisfactory with 0.46-2.01 m RMSE. HEC-RAS simulation results at 100-year RRP (484 mm d⁻¹ rainfall) flood map affected mostly residential buildings. Among the 10 RBs, it was worth-noting that Aunugay RB having only 14.39 km² flood area affected 1,912 residential buildings within short time period of 1.0 hr. Flood areas also affected 7.00 km² cultivated areas and 4.03 km² clay loam soil. Flood simulations at various rainfall scenarios produce realistic flood maps that fit into calibrated and validated DTM thereby able to accurately locate flood hazards affecting AAFNR and properties.

1. INTRODUCTION

1.1 Rationale

Cagayan Valley in Region 2 is located in the northeastern part of Luzon Island, Philippines. It is greatly affected by extreme weather conditions regularly. Because it receives almost 20 typhoons per year, floods are common occurrence in many parts of the valley and in its coastal towns. Millions worth of damages result from calamities brought about by typhoons within the decade. Even with the institutionalization of Disaster Risk Reduction among local government units (LGUs), the havoc brought about by typhoons is drastically significant. It is based on these premises that there is a great need to accurately assess and measure the impacts of floods through the use of LiDAR technology which is one of the better alternatives aside from the use of satellite-based images considering its ability to generate high resolution topographic map such as the digital terrain model (DTM) and land cover map such as the digital surface model (DSM) which can extract more features such as rivers, roads, buildings and other natural resources.

1.2 State of the Art/Problem Analysis

In recent years, earth surface height data has become a vital component of many geospatial planning strategies and is widely used by government agencies and the commercial sector for a variety of applications from flood risk modeling to urban development. LiDAR technology presents an alternative solution to the acquisition of spatial information unanswered by aerial photography or satellite imagery (Shan, J. and Toth, C.K. 2018; Li, Z. et al. 2008). The coverage and accuracy of topographic data extracted by this system, complemented by the features detected by an onboard digital aerial camera, provides rich information that would greatly benefit agencies using spatial data (Figure 1).

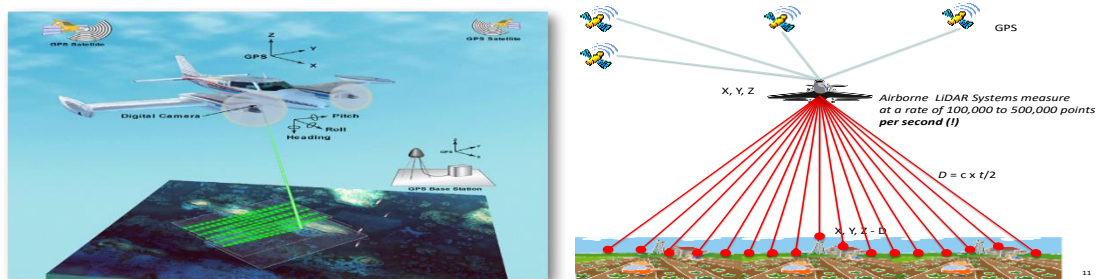


Figure 1. The Light Detection and Ranging (LiDAR) sensor mounted in a low-flying plane to capture point-cloud data (up to 500,000 points sec^{-1}) and sub-meter resolution orthophoto.

Before such data could be utilized, the raw data collected from the LiDAR mission flight need to undergo various processing steps to obtain information that are critical input to the calibration and validation of flood models for the watershed area (Elmqvist, M. 2001). The enormous amount of LiDAR data needs to be filtered to extract the Digital Terrain Model (DTM) from the Digital Surface Model (DSM) (Sithole, G. and Vosselman, G. 2004). The DTM is the boundary surface between the solid ground and the air, which is also the surface of superficial water run-off. This is the surface needed to model the geometry of the watershed and the floodplain. The DSM is used in presenting the impact of flooding to man-made and natural features on the floodplain. Features significant to flood modeling and flood impact assessment such as buildings, forest cover, roads and river network also need to be extracted (NDEP 2004).

LiDAR is a rapid geospatial data acquisition system that can output robust datasets and collect data in a wide range of conditions. But just like any other data acquisition system, it is subject to random and systematic errors (Liu, X. 2011). Hence, conducting data verification and validation ensures that raw and derived data pass the quality requirements of succeeding projects and applications (ASPRS LIDAR Committee 2004). It also ensures the integrity, correctness and completeness of the data through consistent checking.

The use of calibrated and validated LiDAR-derived elevation datasets (DTM/DSM) in flood modeling and hazard assessment offers many advantages. The significantly higher spatial resolution and vertical accuracy of LiDAR-derived elevation data provides clear advantages for use in delineating lands subject to flooding as it allows a detailed representation of flooded areas while avoiding over or under estimation in the delineation of hazard areas. Moreover, LiDAR-derived elevation, especially DSM, contains important topographic features such as roads, buildings, river banks and dykes that have great effect on flow dynamics and flood propagation. These features are absent in low resolution non-LiDAR-derived elevation data such as Landsat or SRTM satellite images. Using the LiDAR-derived elevation data in in flood modeling, accounts for the effects of extracting more features thereby increasing the accuracy and closeness to reality of the simulated flood hazard maps (Santillan, J.R. 2013).

1.3 Objective

This paper aims to show the accuracy of a new flooding simulation system, based on light detection and ranging (LiDAR)-derived elevation data such as digital terrain and surface models (DTM and DSM), capable of predicting the impacts to agriculture, aquatic, forestry and natural resources (AAFNR) and properties at specified rainfall scenarios.

2. METHODOLOGY

2.1 LiDAR Data Processing

Editing, mosaicking, bathymetric data burning of bare earth DTM and feature extraction and attribution of buildings, roads and bridges and waterbodies using DSM were done.

2.2 LiDAR DEM Validation

Validation was done by getting the difference in elevation of each checkpoint and its corresponding LiDAR data point. The RMSE was then computed using the differences in elevation of all the checkpoints, as well as the vertical accuracy at 90% confidence interval which was equal to 2.0 RMSE.

2.3 Topographic and Hydrographic Surveys

Information on river, lake and sea bed topography and geometry was necessary in flood modeling. However, these features were poorly represented in LiDAR data due to low penetration of the light signals in water. To supplement this information, river profile, cross-section and bathymetric data were collected using GNSS, total station, and echo-sounder and integrated (“embedded”) into the LiDAR data for use in flood modeling.

2.4 Hydrological Measurements

Rainfall, water level and discharge measurements were done in the floodplain to be used in flood model calibration and validation. Rain gauges, water level sensors, and velocity meters were installed for at least one month during the rainy season. Cross-section measurements were done so that the rate of discharge can be computed. The water level and the computed discharge were used in generating rating curves for water level forecasting. Rain event/high flow during the Monsoon Rain on December 26-30, 2016 was used to calibrate the HEC-HMS model. The hydrologic data collection covered the period 26 December 2016 00:00 until 28 December 2016 07:30.

Hydrologic data set included the river velocity (using mechanical velocity meter), river water depth using data logging depth gauge) and rainfall downloaded from the web portal of Philippine E-Science Grid- ASTI collected from data logging sensor of automatic rain gauge (ARG) located in Barangay Santa Clara (**Figure 2**) installed by the Department of Science and Technology-Advanced Science and Technology Institute (DOST-ASTI).

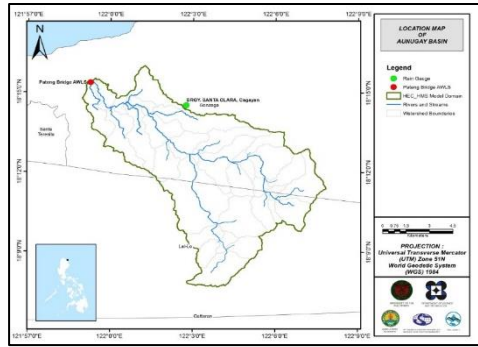


Figure 2. The location of ARG in Barangay Sta. Clara, Gonzaga, Cagayan.

Total rainfall from Barangay, Santa Clara ARG was 91 mm. It peaked to 7.0 mm on 27 December 2016 7:15 PM. The lag time between the peak rainfall and discharge was 8 hr and 50 min (**Figure 3**).

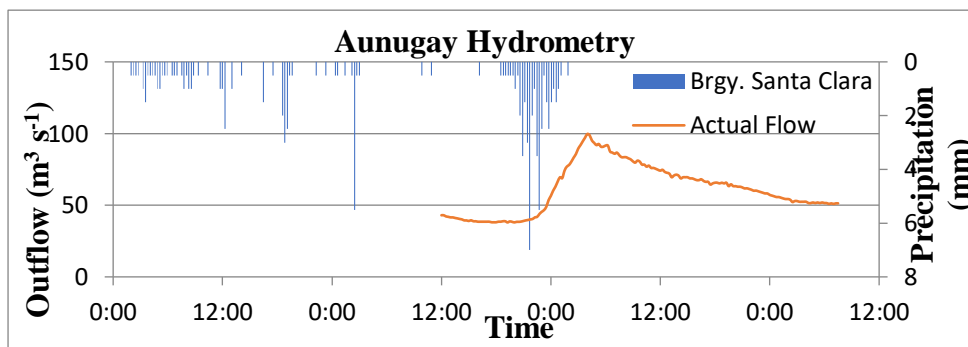


Figure 3. Rainfall and outflow data used for modeling.

A rating curve (H-Q curve) was developed at Pateng Bridge, Pateng, Gonzaga, and Cagayan with geographic coordinates 18.3°N, 122°E. It gives the relationship between the observed water levels (H) from the depth gauge installed during field validation and outflow (Q) at this location. The rating (H-Q) curve generated from the relationship of the observed flow and water level using the equation:

$$Q = aH^n$$

Where: Q=Discharge ($m^3 s^{-1}$) and bridge cross-section area (A) filled with river water \times velocity (V) of river water at the bridge measured using flow meter at the bridge. H = Gauge height (reading from Aunugay Bridge depth gauge sensor); a, n = Constants

The Rating (H-Q) Curve of Aunugay River measured at Pateng Bridge was expressed as $Q = 9E-14e^{2.9109x}$ (**Figure 4**).

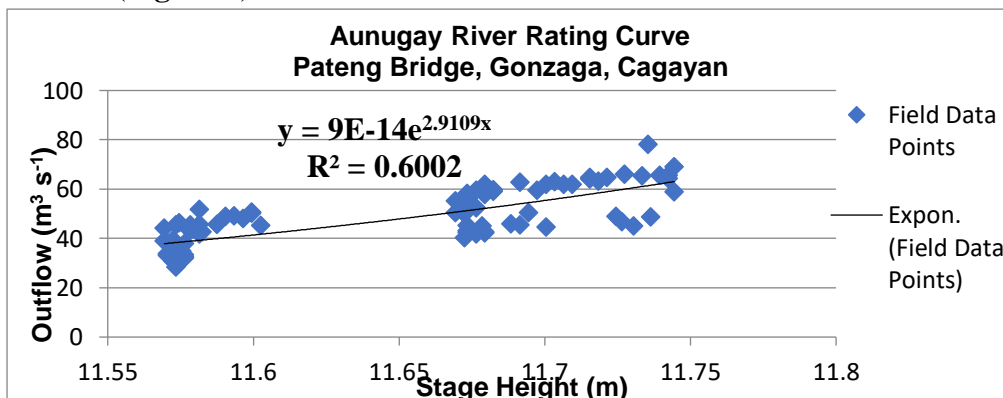


Figure 4. H-Q Curve of the HEC-HMS model.

2.5 Flood Modelling and Simulation

The flood model of each RB was developed according to the spatial framework for flood analysis described earlier. The upstream watersheds and the floodplains of the RBs were delineated using watershed delineation algorithm in ArcGIS software using synthetic aperture radar (SAR) DEM and the calibrated and validated LiDAR DTM. The hydrological model for the upstream watersheds were developed using the Hydrologic Engineering Center-Hydrologic Modeling System (HEC-HMS) software. Landcover parameters of the HEC-HMS model were derived through analysis of landcover shape file from the Department of Agriculture-Bureau of Soil and Water Management (DA-BSWM). Other parameters of the model were set to initial values and were adjusted during calibration. After calibration, the model was validated with an independent set of rainfall and discharge data. A sample HMS model setup of Aunugay RB is shown in **Figure 5**.

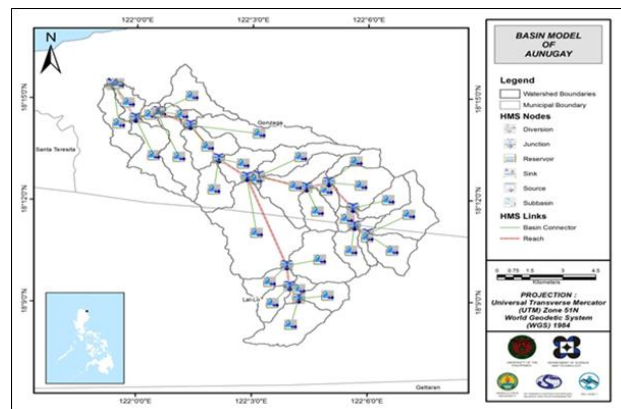


Figure 5. Hydrologic model of Aunugay RB generated using HEC-HMS.

The hydraulic model for the floodplain was developed using the Hydrologic Engineering Center-River Analysis System (HEC-RAS) modeling software. This model utilized cross-section data extracted from the validated LIDAR-derived DTM which was already embedded with river and topographic data. The river bed parameter of the model such as Manning's roughness coefficient (n) was selected based on actual observation. Using the riverbed cross-section data derived from the LiDAR DEM, the HEC-RAS model was generated using the Arc GeoRAS tool of ArcGIS 10.2.2 (**Figure 6**).

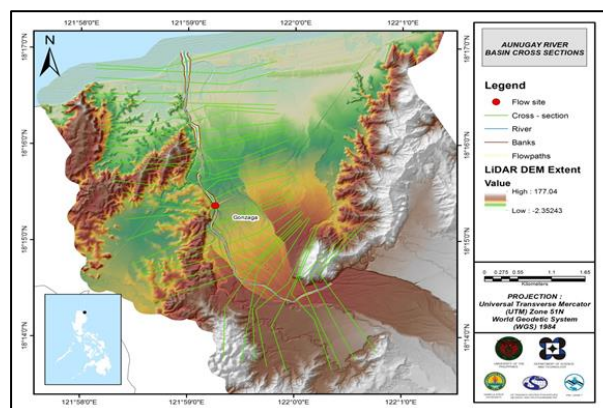


Figure 6. HEC-GeoRAS model, Aunugay RB.

The flood model which was the combination of HEC-HMS and HEC-RAS was used to run actual flood events in the RBs, as well as to simulate flooding due to hypothetical extreme rainfall events at various rainfall return periods.

Data on these hypothetical rainfall events were obtained from the nearest PAGASA Station. The results of the flood simulations were then used to generate water surface elevation grids which were overlaid into the high resolution LiDAR DTM to generate flood hazard maps. HEC-HMS was used to generate discharge hydrographs as inputs into HEC-RAS.

Figure 7 shows the Aunugay River outflow using the Aparri Rainfall Intensity-Duration-Frequency (RIDF) curves in five different return periods (5-, 10-, 25-, 50-, and 100-year) based on the Philippine Atmospheric Geophysical and Astronomical Services Administration (PAGASA) data. The simulation results revealed significant increase in outflow magnitude as the rainfall intensity increased for a range of durations and return periods.

A summary of the total precipitation, peak rainfall, peak outflow and time to peak of the Aunugay discharge using the Aparri RIDF in five different rainfall return periods is tabulated in **Table 1**.

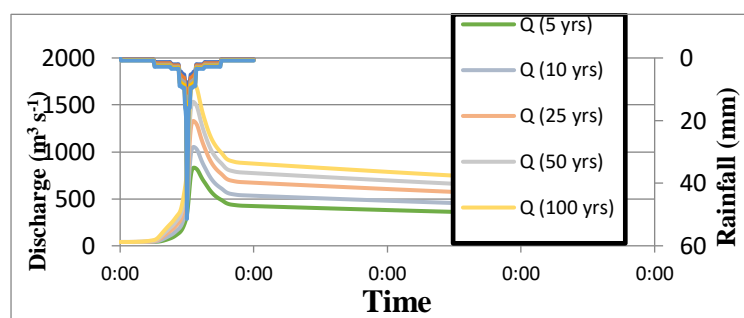


Table 1. RIDF and peak values of rainfall and outflow, Aunugay RB.

RIDF Period	Total Precipitation (mm)	Peak rainfall (mm)	Peak outflow (m ³ s ⁻¹)	Time to Peak
5-Year	252.5	28.5	831.3	1 h, 20 min
10-Year	308.5	34.1	1,052.1	1 h, 10 min
25-Year	379.3	41.1	1,329.2	1 h, 10 min
50-Year	431.9	46.3	1,532.2	1 h, 10 min
100-Year	484	51.4	1,734.4	1 h

Figure 7. Outflow hydrograph at Aunugay Weather Station generated using Aparri RIDF simulated using the calibrated HEC-HMS model.

The HEC-RAS Flood Model produced a simulated water level at every cross-section for every time step for every flood simulation created. The resulting flood map was used in determining the flooded areas such as buildings (residential, commercial, government/ institutional), land use/cover (forests, grasslands, cultivated lands, inland water bodies, mangroves) and soil types (clay, loam, silt, sand) within the floodplains.

2.6 Flood Height Validation

In order to check and validate the extent of flooding in different river systems, there was a need to perform validation survey. From the Flood Depth Maps produced, multiple points representing the different flood depths for different rainfall scenarios were identified for validation. Specified points were identified in a river basin and gathered data regarding the actual flood level based on interviews from the communities using GPS. After which, the actual data from the field were compared to the simulated data to assess the accuracy of the Flood Depth Maps produced. The flood validation consisted of at least 100 points randomly selected all over the floodplain and should have a value equal or less than 2.0 m RMSE.

3. RESULTS AND DISCUSSION

3.1 LiDAR Data Coverage

A total of 6,087.58 km² LiDAR DEM was processed covering the 10 selected RBs in Northeastern Luzon using the major considerations for RB selection such as population, presence of bridge as outlet of rainfall-runoff from the watershed to the floodplains and accessibility/peace and order

situation. As shown in **Figure 8** and **Table 2**, Apayao-Abulug had the largest RB and floodplain area while Ilagan had the highest population in the floodplain.

Table 2. Profile of the ten selected river basins.

River Basin (Location)	Watershed			Floodplain		
	Area (sq km)	No. of Municipalities	No. of Barangays	Area (sq km)	% of Watershed	Population (2015)
1 Apayao-Abulug	2,801.08	20	161	834.20	29.78	19,574
2 Pinacanauan de Ilagan	1,736.69	8	122	813.11	46.82	145,568
3 Pamplona	683.23	7	34	220.52	32.28	8,626
4 Cabicungan (Claveria)	227.53	6	36	230.54	101.32	7,755
5 Amro (Casiguran)	203.93	2	23	103.39	50.70	16,357
6 Aunugay (Gonzaga)	108.58	2	12	44.92	41.37	11,825
7 Baua (Gonzaga)	105.38	1	7	45.75	43.42	2,030
8 Linao (Aparri)	88.42	3	28	191.33	216.38	30,776
9 Tangatan (Sta. Ana)	68.35	1	11	94.34	138.03	24,017
10 Casambalangan (Sta. Ana)	64.39	2	6	23.93	37.17	9,805
Total	6,087.58	52	440	2,602.04		276,333

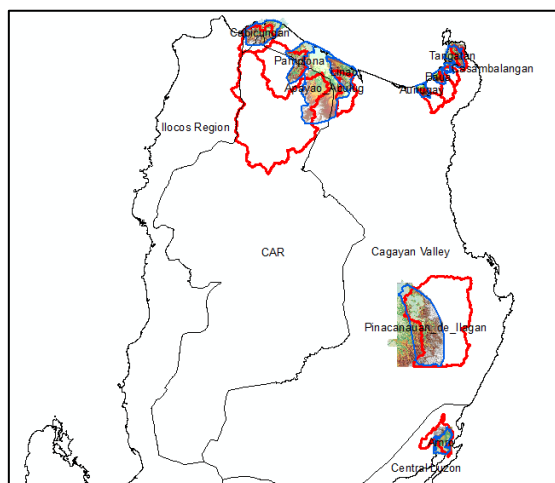


Figure 8. Location map of river basin project sites in Northeastern Luzon.

3.2 Calibrated and Validated LiDAR DEM and Features Extracted

The calibrated and validated LiDAR DEM and features extracted (roads, buildings, waterbodies) for each of the 10 RBs were outputs of editing, mosaicking, bathymetric data burning and feature extraction and attribution using the GIS software. All the calibrated and validated LiDAR DEM passed the 2.0 m RMSE cut-off value with Aunugay RB having the highest accuracy (**Table 3**). A sample output is shown in **Figure 9**.

Table 3. Accuracy of calibrated and validated DEM.

River Basin (Location)	Calibrated DEM (Mosaicked DTM)			Integrated Bathymetric Data into DEM	
	Check Points	Height Difference (meters)	RMSE (meters)	Check Points	RMSE (meters)
1 Apayao-Abulug	1,164	4.07	0.19	27,754	0.25
2 Pinacanauan de Ilagan	4,042	4.07	0.17	26,003	0.54
3 Pamplona	186	4.07	0.84	11,803	0.49
4 Cabicungan (Claveria)	389	5.29	0.11	16,071	0.59
5 Amro (Casiguran)	420	0.75	0.17	8,935	0.19
6 Aunugay (Gonzaga)	9,716	4.07	0.37	4,412	0.12
7 Baua (Gonzaga)	186	4.07	0.20	2,516	0.34
8 Linao (Aparri)	764	4.07	1.29	5,514	0.5
9 Tangatan (Sta. Ana)	526	4.07	0.198	4,036	0.27
10 Casambalangan (Sta. Ana)	275	4.07	0.2	3,732	0.31

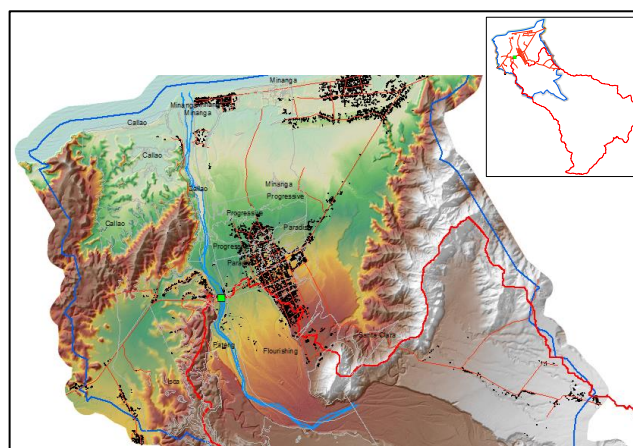


Figure 9. Calibrated and validated DEM and building features in Aunugay RB.

Most of the building features extracted from the DSM in all the 10 RBs were residential ranging from 1,534 (lowest) in Casambalangan to 38,073 (highest) in Apayao-Abulug. Barangay roads were the longest among road networks in all RBs ranging from 14.28 km (shortest) in Casambalangan to 946.77 km (longest) in Apayao-Abulug. Waterbodies were dominated by rivers/streams ranging from 5 (lowest) in Casambalangan and 97 (highest) in Pinacanauan de Ilagan.

3.3 Hydrometry and Rating Curve

After the calibration, **Figure 10** shows the comparison between the actual outflow and the simulated outflow using the HEC-HMS model. **Table 4** presents the accuracy measurements of calibrated HEC-HMS model against the actual observed outflow values.

Table 4. Summary of Efficiency Tests of HEC-HMS Models of the 10 RBs.

River Basin (Location)	r ²	NSE	PBIAS	RSR
1 Apayao-Abulug	0.93	0.77	-12.16	0.48
2 Pinacanauan de Ilagan	0.96	0.93	-2.35	0.26
3 Pamplona	0.97	0.90	-7.13	0.32
4 Cabicungan (Claveria)	0.91	0.88	-3.46	0.34
5 Amro (Casiguran)	0.97	0.96	-2.42	0.19
6 Aunugay (Gonzaga)	0.89	0.88	3.32	0.35
7 Baua (Gonzaga)	0.96	0.85	0.56	0.38
8 Linao (Aparri)	0.91	0.86	-1.41	0.38
9 Tangatan (Sta. Ana)	0.89	0.88	0.49	0.35
10 Casambalangan (Sta. Ana)	0.94	0.92	-8.94	0.28

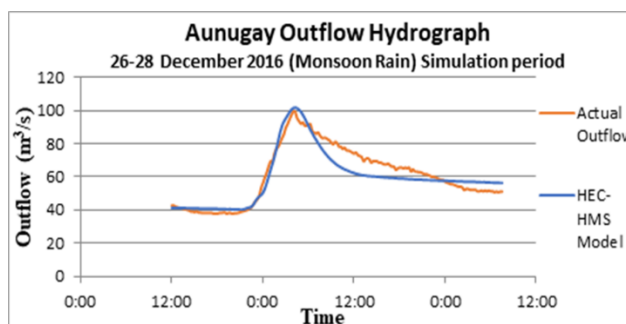


Figure 10. Comparison between observed and HEC-HMS-simulated outflow hydrograph.

The Pearson correlation coefficient (r²) assesses the strength of the linear relationship between the observations and the model. A value close to 1 corresponds to an almost perfect match of the observed discharge and the resulting discharge from the HEC-HMS model. Pamplona and Amro RBs obtained the most desirable r² value of 0.97. The Nash-Sutcliffe (E) assesses the predictive power of the model. The optimal value is 1. Amro RB obtained the best NSE value of 0.96. A positive Percent Bias (PBIAS) indicates a model’s propensity towards under-prediction. Negative value indicates bias towards over-prediction. The optimal value is 0. Tangatan RB had the closest to 0 with PBIAS value of 0.49. The Observation Standard Deviation Ratio, RSR, is an error index. A perfect model attains a value of 0. AMRO RB had the least error index with RSR value of 0.19.

3.4 Accuracy of validated flood depth maps

The highest accuracy obtained was in Linao RB with RMSE value of 0.46 using 232 validation points while the lowest was in Aunugay RB with RMSE value of 2.01 using 178 validation points (**Table 5**). The validation points are displayed with the flood depth map in **Figure 11**.

Table 5. Number of validation points and RMSE of the 10 RBs.

River Basin (Location)	Number of Validation Points	RMSE
1 Apayao-Abulug	293	1.54
2 Pinacanauan de Ilagan	205	1.43
3 Pamplona	197	0.73
4 Cabicungan (Claveria)	274	1.13
5 Amro (Casiguran)	174	1.31
6 Aunugay (Gonzaga)	178	2.01
7 Baua (Gonzaga)	160	1.21
8 Linao (Aparri)	232	0.46
9 Tangatan (Sta. Ana)	226	0.77
10 Casambalangan (Sta. Ana)	196	1.11

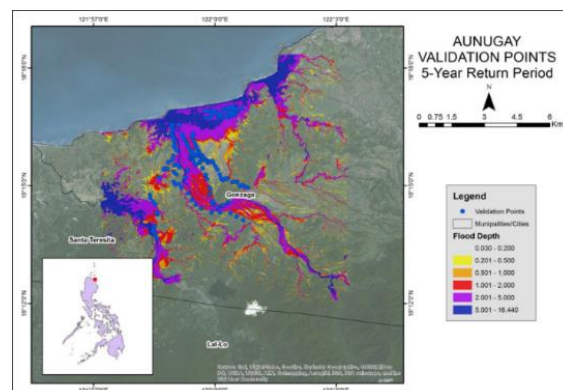


Figure 11. Flood validation points plotted using GPS in the flood depth map.

3.5 Flood simulation

The validated HEC-RAS Flood Models were capable of producing flood hazard maps at various rainfall scenarios (rainfall return periods).

3.5.1 Buildings affected by floods at 100-year rainfall return period. The buildings that will be affected by floods at 100-year rainfall return period with a total rainfall of 484 mm d⁻¹ were mostly residential. It was worth-noting that Aunugay RB having only 14.39 km². Flood area will affect 1,912 residential buildings within short time period of only 1 hr (Table 6). Figure 12 shows the 100-year flood map affecting mostly residential buildings in Aunugay floodplain.

Table 6. Buildings affected by floods at 100-yr rainfall return period.

Name of RB	Watershed Area (sq km)	Floodplain Area (sq km)	% of Watershed	100-yr Return Period (Total rainfall = 427.9 mm; Peak rainfall = 42.9 mm, Peak outflow = 2,162.1 cms)				
				Time to Peak (hrs, min)	Area Flooded (sq km)	Number of Buildings Affected		
						Residential	Commercial	Institutional
Apayao-Abulug	2,801.08	834.20	29.78	11 hrs, 20 min	66.78	3,459	185	169
Pinacanauan de Ilagan	1,736.69	813.11	46.82	3 hrs, 30 min	23.94	2,043	34	64
Pamplona	683.23	220.52	32.28	3 hrs, 40 min	14.41	811	2	21
Cabcungan	227.53	230.54	101.32	1 hr, 10 min	9.31	1,148	10	39
Amro	203.93	103.39	50.70	3 hrs, 50 min	6.37	184	21	19
Aunugay	108.58	44.92	41.37	1 hr	14.39	1,912	57	285
Baua	105.38	45.75	43.42	2 hrs, 20 min	4.18	42	-	-
Linao	88.42	191.33	216.38	9 hrs	27.58	1,055	20	30
Tangatan	68.35	94.34	138.03	2 hrs, 10 min	7.73	287	5	44
Casambalangan	64.39	23.93	37.17	1 hr, 40 min	4.16	218	9	-

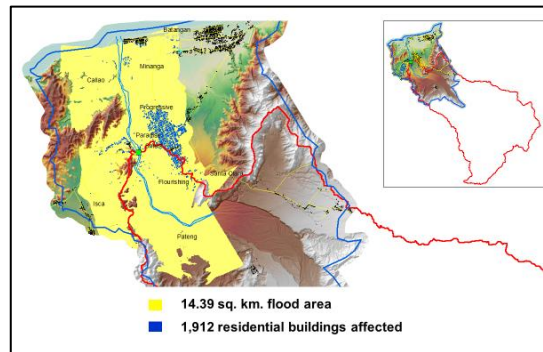


Figure 12. 100-yr flood map affecting mostly residential buildings in Aunugay floodplain.

3.5.2 Land use/cover affected by floods at 100-year rainfall return period. Across land use/cover of most (8 out of 10) RBs, floods affect most cultivated areas (Table 7). Among RBs, Apayao-Abulug had the highest cultivated areas with 47.63 km². Figure 13 shows the 100-year flood map affecting cultivated areas in Aunugay floodplain.

Table 7. Land use/cover affected by floods at 100-yr rainfall return period.

Name of RB	Floodplain Area (sq km)	Time to Peak (hrs, min)	Area Flooded (sq km)	Area (sq km) of Land Use/Cover Affected											
				Inland Water											
				Closed Canopy Forest	Open Canopy Forest	Brushland	Tree Plantation	Cultivated Areas	Area (sq. km.)	No. of Rivers	No. of Creeks	No. of Fishponds	Marshland	Mangrove	Open Areas
Apayao-Abulug	830	11 hrs, 20 min	66.78		3.02	0.27	3.43	47.63	6.35	2	20	47		4.71	1.31
Pinacanauan de Ilagan	810	3 hrs, 30 min	23.94				21.89	2.02	4	1	-				
Pamplona	220	3 hrs, 40 min	14.41		2.71	0.022		2.64	1.96	20	-	6		6.9	0.08
Cabcungan	230	1 hr, 10 min	9.31		1.37		7.29	0.3	3	5	-			0.13	
Linao	190	9 hrs	27.58		0.039	0.3	0.85	14.9	0.51	3	16	29	0.765	9.23	0.38
Amro	100	3 hrs, 50 min	6.37		0.11			4.62	0.42	3	4	-		1.17	
Aunugay	45	1 hr	14.39	0.77	0.41	5.93		7.00	1.54	1	-	-			
Baua	46	2 hrs, 20 min	4.18	0.2	0.32	0.063	0.97	2.35	0.24	1	3	-		0.032	
Tangatan	94	2 hrs, 10 min	7.73		2.05	0.295		5.03	0.12	1	7	-		0.002	0.001
Casambalangan	24	1 hr, 40 min	4.16	0.46	0.33		0.075	3.21	0.31	1	2	4		0.076	

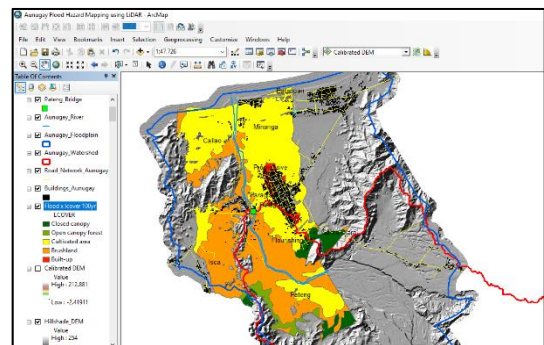


Figure 13. 100-yr flood map affecting 7.0 sq. km. cultivated areas in Aunugay floodplain.

3.5.3 Soils affected by floods at 100-year rainfall return period. Across RBs, floods affect a variety of soil types. Tangatan affects most mountain soils, Linao affects most Zaragosa clay, Apayao-abulug affects most Toran silty clay, and Pamplona affects most Toran loam, Alaminos loam, Bolinao clay loam, San Manuel Silt/Silt loam, San Miguel Silt loam, and Buguey loamy sand (Table 8). Figure 14 shows the 100-year flood map affecting mostly clay loam soils in Aunugay floodplain.

Table 8. Soils affected by floods at 100-yr rainfall return period.

Name of RB	100-yr Return Period (Total rainfall = 427.9 mm; Peak rainfall = 42.9 mm, Peak outflow = 2,162.1 cms)																						
	Time to Peak (hrs, min)	Area Flooded (sq km)	Heavy to n soil (sandier soil)	Zarago (silty clay)	Toran (silty clay)	Alamin (loam)	Alamro (silty clay)	Anaman (clay loam)	Bantay (clay loam)	Bolina (silty clay)	Ilagan (loam)	Rugao (clay loam)	Quiang (silty clay)	Quiang (silty clay)	San Manuel (sandy loam)	San Manuel (silty clay)	Baler (silty clay)	Limnaga (sandy clay)	Baguay (sandy clay)	Hydro- soil	Beach Sand		
Apayao-Abuhad	1 hr, 20 min	66.78		0.93	17.66			3.76						8.81	0.011	3.22	23.21		1.61			2.00	
Pincanauan de Ilagan	1 hr, 30 min	23.94														20.91							
Pamploona	1 hr, 40 min	14.41			0.018	1.08	0.31	0.21							0.45		8.16			2.14			
Cabibangan	1 hr, 20 min	9.31							0.79								4.09						
Linao	1 hr	27.58		0.38	10.07		0.002	0.55		2.48					2.99	1.88			0.18	7.78	1.26		
Amro	1 hr, 50 min	6.37																6.03					
Aunugay	1 hr	14.39	1.9		0.522			4.09	3.09					0.7					1.88	0.980		1.51	
Bace	1 hr, 20 min	4.18	1.61					2.95						0.32	0.087					1.04	0.8	0.009	
Tangatan	1 hr, 20 min	7.73	3.00					0.149							2.7								
Casambalangan	1 hr, 40 min	4.16	2.03					1.58												0.45		0.34	

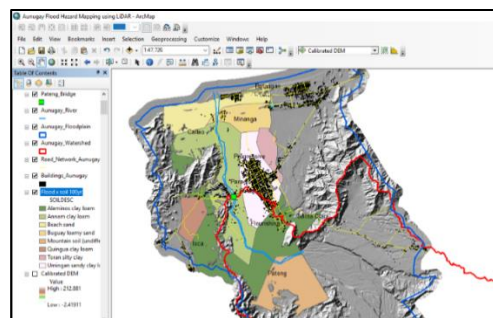


Figure 14. 100-yr flood map affecting 4.0 sq. km. clay loam soils in Aunugay floodplain.

4. CONCLUSIONS AND RECOMMENDATION

Accuracy of the calibrated and validated DEM, features extracted and flood heights in the 10 RBs had all passed the allowable 2.0 m RMSE. The calibrated and validated HEC-HMS models of the 10 RBs obtained satisfactory efficiency test values (r^2 of 0.89-0.97 and NSE of 0.77-0.96 which were close to 1.00, more negative PBIAS and low RSR of 0.19-0.48 which indicated an almost perfect match between simulated and observed outflows). Accuracy of the validated flood heights were satisfactory ranging from 0.46 m for Linao RB in Aparri, Cagayan to 2.0 m for Aunugay RB in Gonzaga, Cagayan.

Outflow time to peak shortens (became faster) as rainfall return periods became longer (5-, 25-, 100-years). Floods affect mostly residential buildings. It was worth-noting that Aunugay RB having only 14.39 km² flood area will affect 1,912 residential buildings within short time period of 1 h. Landuse/landcover mostly affected was 7.00 km² cultivated areas that would affect agricultural facilities and farming systems and waterbodies that would affect aquatic resources and fishery. Soil type mostly affected was clay loam with 4.03 km² area.

These flood hazard maps showing the vulnerability of AAFNR and properties should be mainstreamed in LGU planning and development activities.

REFERENCES

Shan, J. and C.K., Toth 2018. *Topographic laser ranging and scanning: principles and processing*. (1st ed), CRC Press, USA.

Li, Z., Chen, J., Baltsavias, E. 2008. *Advances in photogrammetry, remote sensing and spatial information sciences: 2008 ISPRS Congress Book*. (1st edn), CRC Press, USA.

Elmqvist, M., Jungert, E., Lantz, F., Persson, A., Söderman, U. 2001. *Terrain modelling and analysis using laser scanner data*. *Int Arch Photogrammetry and Remote Sensing* 34: 219-226.

Sithole, G., and G. Vosselman. 2004. *Experimental comparison of filter algorithms for bare-earth extraction from airborne laser scanning point cloud*. *ISPRS J Photogrammetry and Remote Sensing* 59: 85-101.

NDEP, 2004. *Guidelines for digital elevation data*. National Digital Elevation Program (NDEP).

Liu, X. 2011. *Accuracy assessment of LiDAR elevation data using survey marks*. *Survey Rev* 43: 80-93.

ASPRS LiDAR Committee 2004. *ASPRS Guidelines-Vertical Accuracy reporting for LiDAR data*. American Society for Photogrammetry and Remote Sensing.

Santillan, J.R. 2013. *Surveys and measurement technologies for flood control, mitigation and management system*. Applied Geodesy and Space Technology Research Laboratory, Training Center for Applied Geodesy and Photogrammetry, University of the Philippines, Diliman, Quezon City.